

Normal-state reflectivity and superconducting energy-gap measurement of $\text{La}_{2-x}\text{Sr}_x\text{CuO}_4$

Z. Schlesinger, R. T. Collins, and M. W. Shafer

IBM Thomas J. Watson Research Center, Yorktown Heights, New York 10598

E. M. Engler

IBM Almaden Research Center, San Jose, California 95120

(Received 26 June 1987)

We measure the reflectivity of pure and doped polycrystalline $\text{La}_{2-x}\text{Sr}_x\text{CuO}_4$ in the gap region and up to 40000 cm^{-1} ($\approx 5\text{ eV}$). For the doped sample we analyze the reflectivity in terms of a superposition of a metallic a - b plane component and a nearly insulating c -axis component with ordinary phonons. This approach removes several unphysical results obtained assuming a homogeneous surface and allows agreement between the measured infrared and dc properties, which has not been previously obtained. This approach further indicates that our infrared gap signature is dominated by the c -axis contribution and insensitive to the gap in the a - b plane. We estimate the c -axis gap to be $2\Delta \approx 2k_B T_c$, which is small compared to both the isotropic Bardeen-Cooper-Schrieffer prediction and tunneling measurements.

Recently, high-temperature superconductivity has been discovered in metallic oxides in the layered K_2NiF_4 structure,¹ prompting a great deal of research on the properties of these and related compounds. Infrared (ir) measurements are useful both for the study of the superconducting energy gap²⁻⁶ and the normal-state excitations and modes,⁵⁻¹⁰ which may be relevant to the superconductivity. In anisotropic systems such as these one would like to study polarized reflectivity from single crystals, since both the normal-state and superconducting properties are strongly dependent on orientation.¹¹ At the present time, high quality single crystals which are large enough for the ir measurements are not available and considerable effort has been expended in the study of polycrystalline samples. A number of controversies exist regarding both the gap measurement²⁻⁶ and the interpretation of the normal-state reflectivity data⁵⁻¹⁰ in these samples.

In the present work we measure the reflectivity of pure and doped polycrystalline $\text{La}_{2-x}\text{Sr}_x\text{CuO}_4$ over a wide frequency range. In the individual crystallites the conductivity is believed to be much larger in the a - b plane than along the c axis. Reflectivity measurements on single crystals of the isostructural compound La_2NiO_4 exhibit a metallic reflectivity for the incident electric field in the a - b plane, and a nearly insulating response for E parallel to the c axis.¹² Based on these observations we model the reflectivity as a composite spectrum consisting of independent contributions from different crystallite orientations, one metallic contribution from the a - b plane, and one nearly insulating c -axis contribution. This approach enables us to understand the primary features of the reflectivity in terms of ordinary phonon and plasmon contributions, and to obtain for the first time agreement between the measured ir and the dc properties (conductivity and carrier density). We also find that our infrared measurement of the superconducting energy gap is dominated by the contribution from the low reflectivity c axis and is insensitive to the a - b plane gap. Our modeling indicates that this out-of-plane gap is about $2\Delta \approx 2k_B T_c$. This value is substantially less than the gap measured by tunneling¹³

($2\Delta \approx 4k_B T_c$), suggesting the speculation that the out-of-plane gap is smaller than the gap in the a - b plane.

Our $\text{La}_{2-x}\text{Sr}_x\text{CuO}_4$ samples are prepared from nitrate solutions which are converted into oxides and reacted by solid state reaction.¹⁴ They are pressed into pellets which are then annealed and polished. The samples are polycrystalline with characteristic crystallite sizes on the order of $30\text{ }\mu\text{m}$ and no evidence of any preferential orientation. For the pure ($x=0.0$) sample the room-temperature resistivity is about $0.2\text{ }\Omega\text{ cm}$. The doped sample¹⁴ ($x=0.15$) has a holelike carrier concentration of $\approx 2 \times 10^{21}\text{ cm}^{-3}$, a superconducting transition temperature $T_c \approx 35\text{ K}$, and a resistivity which drops from $2.5 \times 10^3\text{ }\Omega\text{ cm}$ at 300 K to $0.8 \times 10^3\text{ }\Omega\text{ cm}$ at 50 K .

Infrared and optical measurements were made using a polarizing interferometer (10 – 300 cm^{-1}), a scanning interferometer (50 – 10000 cm^{-1}), and a grating spectrometer (4000 – 40000 cm^{-1}). The reflectivity of nominally unpolarized radiation was measured at roughly 45° incidence in the interferometers and near normal incidence in the spectrometer.

In Fig. 1 we show the ratio of the reflectivity in the superconducting state to that in the normal state (R_s/R_n) for several temperatures below the superconducting transition temperature. The enhanced low frequency reflectivity is a characteristic signature of superconductivity; however, the rapid drop of R_s/R_n and the region where $R_s/R_n < 1$ are not typical. We will discuss the origin of this unusual behavior following our analysis of the normal-state reflectivity. Note that the large size of the ratio at, for example, 30 cm^{-1} implies a surprisingly low normal-state reflectivity ($R_n < 80\%$).

In Fig. 2, room-temperature reflectivity spectra for polycrystalline samples with $x=0.0$ and $x=0.15$ are shown for frequencies up to 10000 cm^{-1} . Further data (not shown) extending up to 40000 cm^{-1} (5 eV) show only modest changes in reflectivity between 10000 and 40000 cm^{-1} . At the bottom of each part of Fig. 2 we have indicated the transverse optical phonon frequencies required to fit the data. Based on the single-crystal

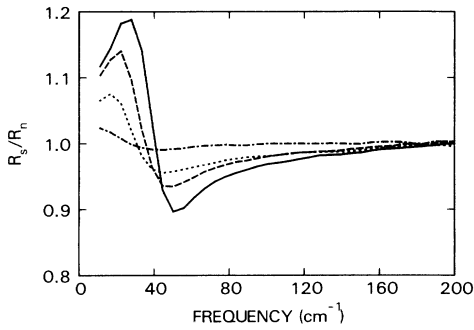


FIG. 1. The measured ratios of the reflectivity in the superconducting state to the reflectivity in the normal state ($T=37$ K) is shown for temperatures in the superconducting state of 13 K (solid line), 25 K (dashed line), 29 K (dotted line), and 33 K (dot-dashed line).

reflectivity measurements on the isostructural compound La_2NiO_4 ,¹² we identify the phonons at 240 and 500 cm^{-1} with lattice vibrations polarized along the c axis, and the phonons at 150, 350, and 680 cm^{-1} with vibrations in the a - b plane. The lack of a - b plane modes in the doped sample is simply a consequence of the metallic screening in the a - b plane, as we will show in more detail below. In the pure sample we expect to see both sets of phonons. The apparent absence (or shift) of the 240- cm^{-1} mode is therefore puzzling.⁹

Attempts to fit or analyze the data for the $x=0.15$ sample assuming reflectivity from a homogeneous medium leads to problems associated with the electronic contribution to the reflectivity. First, the low reflectivity at low frequency implies a dc conductivity much smaller than the measured value.³ Second, the reflectivity below the apparent plasma edge at 5000 cm^{-1} is too low.⁸ (This can be resolved by putting most of the electronic oscillator strength into a gap excitation;¹⁰ however, that approach

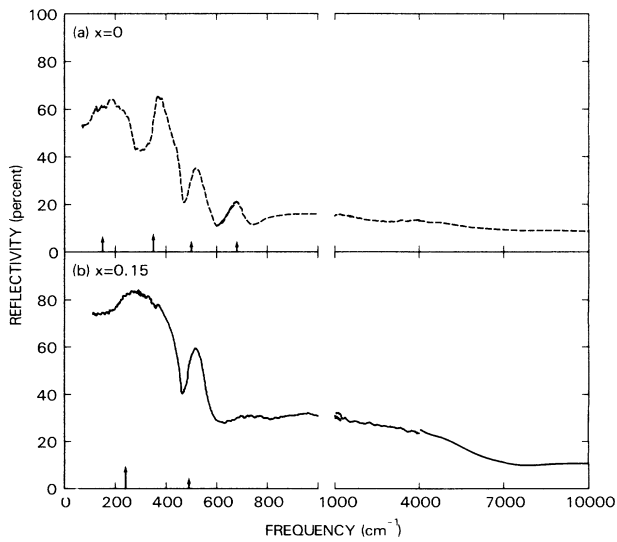


FIG. 2. Measured room-temperature reflectivity spectra for (a) pure LaCuO_4 and (b) $\text{La}_{1.85}\text{Sr}_{0.15}\text{CuO}_4$. Note the change in scale at 1000 cm^{-1} .

contradicts dc conductivity and carrier density results.) Third, the phonon features at ≈ 240 and 490 cm^{-1} are much too strong and sharp to be consistent with any significant metallic screening of these phonon modes.

The preceding observations, as well as our knowledge of the polycrystalline, and highly anisotropic nature of our samples, strongly suggest that we consider the reflectivity as a composite spectrum consisting of contributions from metallic (a - b plane) and nearly insulating (c axis) crystallite orientations. For our modeling we will write

$$R = (1-f)R_{\perp} + fR_{\parallel}, \quad (1)$$

where R_{\perp} is the reflectivity for the incident E field in the a - b plane and R_{\parallel} is the reflectivity for E parallel to the c axis. These individual reflectivities are each calculated from a dielectric function written in the form¹⁵

$$\epsilon(\omega) = \epsilon_{\infty} - \frac{\omega_p^2}{\omega^2 + i\omega/\tau} + \sum_n \frac{\omega_{pn}^2}{\omega_n^2 - \omega^2 - i\omega\Gamma_n}, \quad (2)$$

where $\omega_p' = \omega_p/\epsilon_{\infty}^{1/2}$ is the frequency of the electronic plasma edge, the dc conductivity is $\sigma_{dc} = \omega_p^2\tau/4\pi$, and ω_n , ω_{pn} , and Γ_n are the frequency, strength, and damping of the optic phonon modes (or, in principle, other excitations). Writing the overall reflectivity as a simple average of two independent terms is justifiable when the wavelengths associated with the incident radiation are small compared to the crystallite sizes; however, at lower frequencies the crystallites will begin to screen each other and effective medium-theory-type corrections,¹⁶ which we have not attempted to include, may become significant.

In Fig. 3 we show a reflectivity spectrum calculated for $E \perp c$ using approximate a - b plane phonon parameters, a carrier density of $2 \times 10^{21} \text{ cm}^{-3}$, an effective mass of one, and a conductivity of $10^3 (\Omega \text{ cm})^{-1}$. This spectrum exhibits ordinary metallic behavior with a plasma edge at $\approx 5500 \text{ cm}^{-1}$. The phonons show up only very weakly in this spectrum because of the metallic screening. Also shown in Fig. 3 is a spectrum calculated for $E \parallel c$ using the c -axis phonons ($\omega_n = 240$ and 490 cm^{-1}) and a conductivity which is 100 times less than the value for the a - b plane. For this orientation the gross features of the spectrum are dominated by the phonons and are not very sensitive to the exact value chosen for the conductivity. In Fig. 3(b) we show an average of the two reflectivity spectra in Fig. 3(a) in which we use $f = \frac{1}{2}$. This calculated composite spectrum in Fig. 3(b) mimics the gross features of the measured reflectivity for $x=0.15$ shown in Fig. 2(b). The prominence of the c -axis phonon features arises naturally in this approach, since they are not screened by the free carriers which move primarily in the a - b plane. The low reflectivity at low frequency is also simply accounted for; however, in this region the wavelength of the radiation is longer than typical crystallite dimensions and effective medium-theory¹⁶ corrections to Eq. (1) may be important. This is, of course, a greatly oversimplified modeling of a complex problem, and the choice of $f = \frac{1}{2}$ (rather than $\frac{1}{3}$) is made largely by default since we do not have an *a priori* knowledge of what f should be. This subsumes the much larger question of how one analyzes the measured reflectivity from highly anisotropic, unaligned polycrystalline samples, to which we refer in the

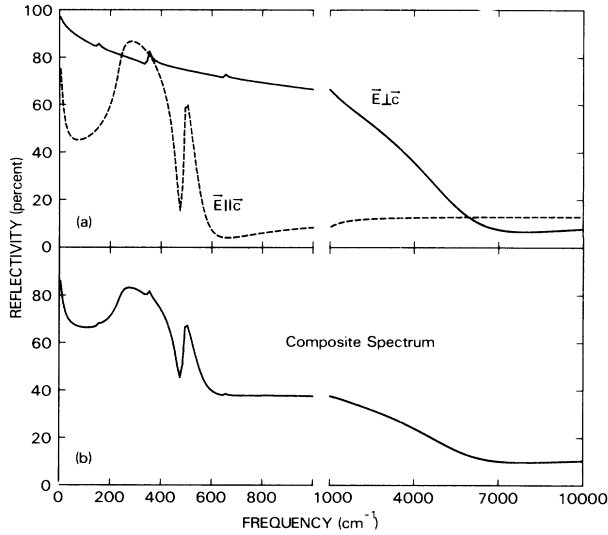


FIG. 3. (a) Calculated reflectivity spectra are shown for a hypothetical single crystal of $\text{La}_{1.85}\text{Sr}_{0.15}\text{CuO}_4$ for $\text{E}\parallel\text{c}$ and $\text{E}\perp\text{c}$. (b) The average of the two spectra in (a) is shown. (Parameters used in the calculation are the following for $\text{E}\perp\text{c}$: $\omega_p = 13000 \text{ cm}^{-1}$, $\tau^{-1} = 3000 \text{ cm}^{-1}$, $\epsilon_\infty = 4.5$, $\omega_1 = 150 \text{ cm}^{-1}$; $\omega_{p1} = 300 \text{ cm}^{-1}$, $\Gamma_1 = 10 \text{ cm}^{-1}$; $\omega_2 = 350 \text{ cm}^{-1}$, $\omega_{p2} = 500 \text{ cm}^{-1}$, $\Gamma_2 = 10 \text{ cm}^{-1}$, and $\omega_3 = 680 \text{ cm}^{-1}$, $\omega_{p3} = 200 \text{ cm}^{-1}$, $\Gamma_3 = 10 \text{ cm}^{-1}$. For $\text{E}\parallel\text{c}$: $\omega_p = 1300 \text{ cm}^{-1}$, $\tau^{-1} = 3000 \text{ cm}^{-1}$, $\epsilon_\infty = 4.5$; $\omega_1 = 240 \text{ cm}^{-1}$, $\omega_{p1} = 900 \text{ cm}^{-1}$, $\Gamma_1 = 40 \text{ cm}^{-1}$, and $\omega_2 = 490 \text{ cm}^{-1}$, $\omega_{p2} = 200 \text{ cm}^{-1}$, and $\Gamma_2 = 10 \text{ cm}^{-1}$).

next paragraph.

In the picture presented here we associate the reflectivity drop near 5000 cm^{-1} with an ordinary Drudelike a - b plane plasma edge. Other researchers have inferred the existence of a ~ 0.5 -eV (4000-cm^{-1}) mode from similar data.¹⁰ The question of the existence of such a mode is an important and subtle one which depends critically on both the data and data analysis. Of particular importance is the ability to extract from data on polycrystalline samples the pure a - b plane and c -axis reflectivities. The existence of the 0.5 -eV mode is then inferred when the magnitude of the a - b plane reflectivity below 4000 cm^{-1} is too small to be fit by the Drude model.¹⁷ The distribution of oscillator strength between the Drude and 0.5 -eV peaks is very sensitive to the absolute value of this reflectivity. With our polycrystalline samples we do not feel that we can perform this analysis with sufficient accuracy to determine the strength of the 0.5 -eV mode. We therefore take the conservative point of view that for $x = 0.15$ most of the dopant-induced oscillator strength is in the Drude term, and the existence and strength of the 0.5 -eV mode remain to be established (presumably by data from single-crystal samples). Although we find no compelling evidence for an 0.5 -eV mode based on the $x = 0.15$ spectrum, data at lower doping,⁸ which show a gradual growth in the reflectivity just below $\approx 5000 \text{ cm}^{-1}$ as a function of x , may indicate a doping-induced electronic excitation in this vicinity. We note that the free-carrier plasma frequency reaches this frequency range at about the doping for which the highest T_c 's occur.

Previous researchers⁷ have been unable to fully under-

stand the origin of the substantial drop in reflectivity near 500 cm^{-1} ; however, with the aid of the La_2NiO_4 data¹² we can confidently identify this feature with the c -axis phonons. The high reflectivity between ≈ 250 and 500 cm^{-1} for the $\text{E}\parallel\text{c}$ axis spectrum is associated with the 240-cm^{-1} mode and the drop in reflectivity near 500 cm^{-1} (which is roughly coincident with the 490-cm^{-1} phonon mode) is due to a zero crossing of $\epsilon_1(\omega)$ which corresponds to a longitudinal phonon frequency [i.e., a peak of $\text{Im}(\epsilon^{-1}(\omega))$]. The substantial separation between the transverse phonon at 240 cm^{-1} and its longitudinal counterpart at $\approx 500 \text{ cm}^{-1}$ reflects the substantial strength of this mode (900 cm^{-1} , which corresponds to effective charge $e^* \approx 9$ for effective reduced mass $M^* = 16$). This strong 240-cm^{-1} mode is present in both metallic La_2NiO_4 (Ref. 11) and doped $\text{La}_{2-x}\text{Sr}_x\text{CuO}_4$.

In the K_2NiF_4 structure the c -axis phonons have $\Gamma_2^-(A_{2u})$ symmetry, in which case there are three infrared active phonons.¹⁸ From the $\text{La}_{2-x}\text{Sr}_x\text{CuO}_4$ reflectivity data we extract c -axis phonon frequencies of 490 cm^{-1} , 345 cm^{-1} (a very weak mode), and 240 cm^{-1} (a very strong mode). The upper two modes are associated with asymmetric stretches of the Cu-O bond, while in the lowest (240-cm^{-1}) mode the oxygen octahedra move in opposition to their lanthanum cage.¹⁸ The unusually large strength of this latter mode, which is about three times larger than that of the corresponding mode in K_2MnF_4 , is probably associated with the high ionic charges ($+3$ and -2) of the La and O. This strong mode, and the c -axis phonons, in general, provide interesting candidates for superconductivity mediation since they are not screened at the dopant concentrations for which the highest T_c 's occur, and they become screened at higher dopant concentration⁷ as T_c begins to drop.

Let us now consider the implications of our model for the interpretation of the superconducting energy gap measurement in Fig. 1. We calculate the reflectivity in the superconducting state using a Mattis-Bardeen conductivity in place of the Drude term in Eq. (2). We are constrained to use the same mass (conductivity) anisotropy in the normal and superconducting states since relaxing that condition introduces a number of problems, especially concerning the conductivity sum rules.

In Fig. 4(a) the calculated ratio of the superconducting to normal reflectivity is shown for the incident electric field in the a - b plane and using a normal-state conductivity of $\sigma_n = 1.5 \times 10^3 (\Omega \text{ cm})^{-1}$ and a superconducting energy gap of $2\Delta = 40 \text{ cm}^{-1}$. For this metallic orientation the ordinary gap signature of a dirty superconductor is obtained. The calculated ratios of R_s/R_n are also shown for E parallel to the c axis with a mass anisotropy of 40 (i.e., using $\sigma_n = 38 (\Omega \text{ cm})^{-1}$). This calculated c -axis gap spectrum exhibits the rapid drop in R_s/R_n and the substantial overshoot region (where $R_s/R_n < 1$) observed in the experiment (Fig. 1). The ratio for the c axis is much larger than for the a - b plane, and will therefore dominate an average constructed to model the response of our unoriented composite samples. Thus, we conclude that our infrared gap measurement is selectively sensitive to the c -axis gap and almost completely insensitive to the gap in the a - b plane. This is a simple consequence of the low

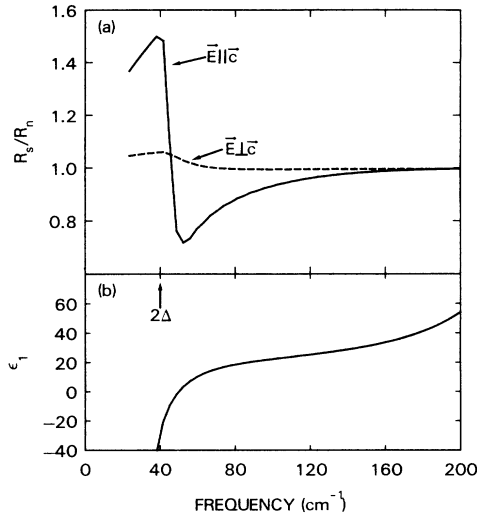


FIG. 4. Calculated ratios of the superconducting to normal reflectivity are shown for $\mathbf{E} \perp \mathbf{c}$, and for $\mathbf{E} \parallel \mathbf{c}$. The values of $\epsilon_1(\omega)$ in the superconducting state are shown in (b).

value of R_n for $\mathbf{E} \parallel \mathbf{c}$.

As first shown by Bonn *et al.*⁶ the rapid drop in R_s/R_n is due to a zero crossing of $\epsilon_1(\omega)$ in the superconducting state [Fig. 4(b)]. They also state that this drop occurs at a substantially lower frequency than 2Δ , and that this depends critically on the relative strengths of the Mattis-Bardeen and phonon contributions to $\epsilon_1(\omega)$ at low frequency. Bonn *et al.*,⁶ however, substantially overestimate the phonon contributions to $\epsilon_1(\omega)$, obtaining a value for $\epsilon_1(0)$ about four times larger than our c -axis value (~ 20) and the La_2NiO_4 single crystal value. The discrepancy occurs because they have not removed the 240-cm^{-1} phonon from the metallic screening of the a - b plane in their analysis and hence overestimate its strength and its

Lydanne-Sachs-Teller residue which dominates the normal state $\epsilon_1(0)$. In the calculation of Fig. 4(a) we find that the reflectivity drop and 2Δ are essentially coincident. To obtain a substantial separation between 2Δ and the drop in R_s/R_n one would require an even smaller conductivity than we have used in Fig. 4(a), which would give poorer qualitative agreement with the measured spectrum (Fig. 1). Comparing the calculated spectrum in Fig. 4(a) with the measured spectrum in Fig. 1, we interpret our gap measurement at $T \approx 13$ K as implying a c -axis gap of about 40 cm^{-1} ($2\Delta \approx 2k_B T_c$) and containing virtually no information regarding the gap in the a - b plane.

These results naturally raise questions regarding the possible anisotropy of the energy gap and of other aspects of the finite frequency conductivity in the superconducting state. Particularly since we have shown that the ir measurement is primarily sensitive to the c -axis gap, one can speculate that the discrepancy with the tunneling gap ($2\Delta \approx 4k_B T_c$) is associated with gap anisotropy (the tunneling measurement may pick up the larger a - b plane gap). Hopefully these questions will be answered by polarized measurements from single crystal samples in the not too distant future.

In conclusion, we have studied the reflectivity of pure and doped ($x = 0.15$) $\text{La}_{2-x}\text{Sr}_x\text{CuO}_4$ from the superconducting energy gap region to 40000 cm^{-1} . We analyze the data in terms of superposition of distinct contributions of $\mathbf{E} \parallel \mathbf{c}$ and $\mathbf{E} \perp \mathbf{c}$ axis orientations. This approach removes previously noted inconsistencies between ir conductivity and the measured carrier density and dc conductivity. Our analysis indicates that the drop in reflectivity at $\sim 5000\text{ cm}^{-1}$ is primarily associated with the a - b plane plasma edge, while the prominent structure in the reflectivity below $\sim 800\text{ cm}^{-1}$ is associated with unscreened c -axis phonons. The analysis of the superconducting gap region shows that our infrared measurement is sensitive only to the c -axis gap. We estimate this out of plane gap to be $2\Delta \approx 2k_B T_c$.

¹J. G. Bednorz and K. A. Müller, *Z. Phys. B* **64**, 189 (1986); J. G. Bednorz, M. Takashige, and K. A. Müller, *Europhys. Lett.* **3**, 379 (1987).
²Z. Schlesinger, R. L. Greene, J. G. Bednorz, and K. A. Müller, *Phys. Rev. B* **35**, 5334 (1987).
³P. E. Sulewski, A. J. Sievers, R. A. Buhrman, J. M. Tarascon, and L. H. Greene, *Phys. Rev. B* **35**, 5330 (1987).
⁴U. Walter, M. S. Sherwin, A. Stacy, P. L. Richards, and A. Zettle, *Phys. Rev. B* **35**, 5327 (1987).
⁵P. E. Sulewski, A. J. Sievers, R. A. Buhrmans, J. M. Tarascon, L. H. Greene, and W. A. Curtin, *Phys. Rev. B* **35**, 8829 (1987).
⁶D. A. Bonn, J. E. Greedan, C. V. Stager, T. Timusk, M. Doss, S. Herr, K. Kamaras, C. Porter, D. B. Tanner, J. M. Tarascon, W. R. McKinnon, and L. H. Greene, *Phys. Rev. B* **35**, 8843 (1987).
⁷Z. Schlesinger, R. T. Collins, and M. W. Shafer, *Phys. Rev. B* **35**, 7232 (1987).
⁸S. Tajima, S. Uchida, S. Tanaka, S. Kambe, K. Kitazawa, and K. Fueki, *Jpn. J. Appl. Phys. Lett. Part 2* **26**, L432 (1987).
⁹H. Sawada, Y. Saito, T. Iwazumi, R. Yoshizaki, Y. Abe, and E. Matsuura, *Jpn. J. Appl. Phys. Lett. Part 2* **26**, L426 (1987).

¹⁰J. Orenstein, G. A. Thomas, D. H. Rapkine, C. G. Bethea, B. F. Levine, R. J. Cava, E. A. Rietman, and D. W. Johnson, *Phys. Rev. B* **36**, 729 (1987).
¹¹T. R. Dinger, T. K. Worthington, W. J. Gallagher, and R. L. Sandstrom, *Phys. Rev. Lett.* **58**, 2687 (1987); T. K. Worthington, W. J. Gallagher, and T. R. Dinger (unpublished).
¹²J.-M. Bassat, P. Odier, and F. Gervais, *Phys. Rev. B* **35**, 7126 (1987).
¹³See, e.g., J. R. Kirtley, C. C. Tsuei, S. I. Park, C. C. Chi, J. Rozen, and M. W. Shafer, *Phys. Rev. B* **35**, 7216 (1987).
¹⁴T. Penny, M. W. Shafer, B. L. Olson, and T. S. Plaskett (unpublished).
¹⁵F. Wooten, *Optical Properties of Solids* (Academic, New York, 1972).
¹⁶See, for example, *Electrical Transport and Optical Properties of Inhomogeneous Media*, edited by J. C. Garland and D. B. Tanner (AIP, New York, 1978).
¹⁷S. Tajima, S. Uchida, A. Masaki, H. Takagi, K. Kitazawa, S. Tanaka, and A. Katsui, *Phys. Rev. B* **32**, 6302 (1987).
¹⁸K. Strobel and R. Geick, *J. Phys. C* **9**, 4223 (1976).